AIMS Materials Science, 4(2): 383-390.
DOI: 10.3934/matersci.2017.2.383
Received: 28 December 2016
Accepted: 19 February 2017
Published: 21 February 2017

http://www.aimspress.com/journal/Materials

Research article

Interaction between magnetic nanoparticles in clusters

Andrea Ehrmann [1,*] and Tomasz Blachowicz [2]

[1] Faculty of Engineering and Mathematics, Bielefeld University of Applied Sciences, 33619 Bielefeld, Germany
[2] Institute of Physics—Center for Science and Education, Silesian University of Technology, 44-100 Gliwice, Poland

* **Correspondence:** Email: andrea.ehrmann@fh-bielefeld.de; Tel: +49-521 106-70254; Fax: +49 521 106-7190.

Abstract: Micromagnetic simulations are often used to model the magnetic properties of nanoparticles, depending on their shape and dimension as well as other parameters. Due to the significant increase in computing time for large-scale models, simulations are regularly restricted to a single magnetic nanoparticle. Applications in bit-patterned media etc., however, necessitate large clusters of nanostructures. In our recent works, the deviations of magnetic properties and magnetization reversal processes, comparing single nanoparticles and small clusters, were investigated using the micromagnetic simulation OOMMF. The studies concentrated on a special fourfold shape which has been shown before to offer four stable states at remanence, allowing for creating quaternary bit-patterned media with two bits storable in one position. The influence of downscaling was examined by varying the sample dimensions without changing the particle shape. The results show that in case of the special square nanostructures under investigation, the largest nanoparticles experience the strongest effect by being included in a cluster, while the technologically more relevant smaller nanoparticles have similar magnetic properties and identical magnetization reversal processes for single and clustered particles.

Keywords: micromagnetic simulation; magnetic nanoparticles; nanoparticle cluster; OOMMF; stable intermediate state; lithography

1. Introduction

Magnetic nanoparticles are of great interest in recent research due to their possible applications

in magnetic storage devices, MRAM (magnetoresistive random access memory), logical circuits, or magnetic quantum cellular automata [1–5]. For higher memory capacity, bit-patterned media with self-assembled magnetic particle arrays can be used instead of conventional thin film systems [6]. Amongst these nanostructures, rings are of special interest due to stray fields being minimized in them. The flux-closed vortex states occurring in such rings can represent different information [7,8,9]; however, differentiating between them usually necessitates new technologies [8,10–13].

In former publications, we have thus reported in detail the magnetic properties and magnetization reversal processes in fourfold or higher-order nanostructured rings from magnetic material, represented by nanowires building squares [14–18] or "walls" as they can be produced by lithographic processes [19]. Depending on shape and dimension as well as material and angular orientation of the external magnetic field, such nanoparticles can show four or even more stable magnetic states at remanence, correlated with exotic magnetic states, such as different onion states, horseshoe or vortex states. Such stable intermediate states are often found in exchange bias systems in simulation and experiment [20,21] but can also occur in ferromagnetic nanoparticles of special shapes. It was found, e.g., that square nanowire rings of four iron (Fe) wires with diameter 10 nm and length 70 nm and with overlapping ends showed magnetization reversal processes via stable intermediate onion states over a broad angular range [17]. By varying the diameters of the crossed wires between 6 nm and 20 nm and the lengths between 30 nm and 70 nm, simulations showed different horseshoe and vortex states [14]. The influence of the relative orientation of the nanowires, especially the amount and place of crossing, was also investigated. Both parameters were found to be crucial for the possible existence of stable intermediate states [16]. In a sixfold wire system with half-balls as corner connections, even more possible magnetic states were found, correlated with one or two steps in the hysteresis loop; however, most of these states were instable so that this approach was not followed further [15]. Changing the material from iron to cobalt, a much broader variety of magnetization reversal mechanisms and magnetic states was found especially in an angular region around 0°, combined with the frequent existence of domain-wall states [18]. These states, however, were less stable than those simulated in iron systems. Stability of lithographically produced open squares with different corner solutions was also modelled for Fe particles of diameter 400 nm. It was found that typical rounded corners, occurring naturally in the lithography process, resulted in strong deviations of the coercive fields [19]. In spite of these problems, square nanowall or nanowire particles are of high interest for the development of magnetic data storage media since they offer the possibility to create quaternary magnetic memories, with each storage position storing two or more bits [17] and thus increased overall storage capacity.

While this finding has been proven for a broad range of parameters for single nanoparticles, the question arose how clustering several nanoparticles would influence the magnetic properties of these special magnetic particles. This is why in the recent paper simulations of fourfold magnetic nanoparticles of different dimensions are analyzed, separately as single objects and additionally as clusters, allowing comparing their coercive fields and magnetization reversal mechanisms.

2. Materials and Method

Magnetic nanostructures were investigated using the micromagnetic simulator OOMMF (Object Oriented MicroMagnetic Framework) [22], based on finite differences (i.e., discretizing space into

small cuboids) and the Landau-Lifshitz-Gilbert (LLG) equation of motion [23]. The simulation parameters were: material Py (permalloy), mesh size 5 nm, damping coefficient 0.05, anisotropy constant $K_1 = 0.5 \times 10^3$ J/m^3, exchange constant $A = 1.05 \times 10^{-11}$ J/m, and saturation magnetization $M_s = 796 \times 10^3$ A/m [24,25,26]. The external field is varied between −200 mT and 200 mT parallel to the sample plane. The sample orientation is varied between 0° (i.e., the external magnetic field parallel to the x-axis of the sample) and 180° in steps of 5°.

The samples under simulation are depicted in Figure 1, showing a single particle as well as a cluster of 4 × 4 particles interacting with each other through their demagnetization fields. Lateral dimensions for the single particles were chosen as 120 nm, 200 nm and 400 nm, identically to real samples investigated in former projects [27,28] and being typical in recent lithographic approaches [27]. The free space between the particles in the clusters was chosen identical to the respective particle width. For a cluster of 4 × 4 objects, the whole structured areas had thus lateral dimensions between 960 nm and 3200 nm side length. The sample height was always 5 nm which is not too high for lithography processes and thus a usual layer thickness for such nanoparticles.

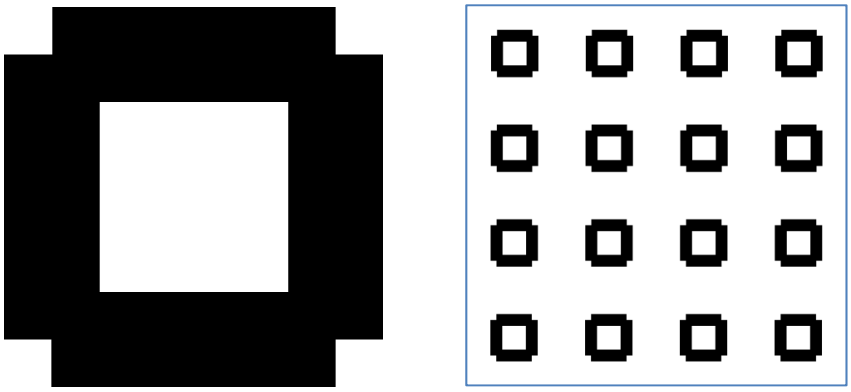

Figure 1. Sample under investigation, used as single particle (left panel) or 4 × 4 cluster (right panel, scaled).

3. Results and Discussion

For the largest particle under investigation with 400 nm width, Figure 2 depicts the results of simulations for a single object and a cluster of 4 × 4 particles. Comparing both graphs, it is visible that for most in-plane angles, the coercive fields are approximately equal, while around the easy axes at 45° and 135°, deviations between both situations occur. For applications in bit-patterned media, however, utilizing the doubled amount of stable states at remanence is only possible in an angular region between max. 5° and 20° [29]. The particle interactions around 45° do thus not raise difficulties in the technologically interesting area. They can be attributed to starting magnetization reversal in the corners of the single magnetic particles, triggered by the interactions with neighboring particles, allowing for easier reversal of a complete side of the nanoparticles. These states with one or two of the corner regions already changing magnetization orientations can only be found in the largest particles due to the necessary area to show coherent magnetization orientation.

Smaller particles may nevertheless be influenced more significantly by interactions between neighboring magnetic objects due to the reduced distances between them. Figure 3 shows the

simulated coercive fields for a single particle of 200 nm side length and the respective 4 × 4 cluster.

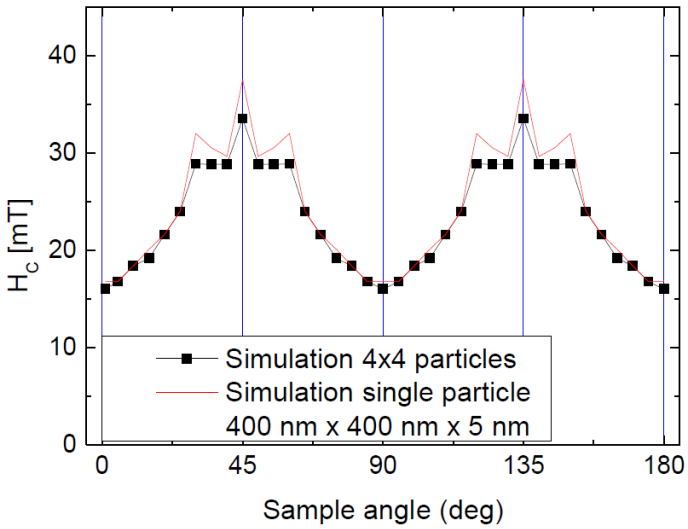

Figure 2. Simulation of single particle with 400 nm side length and 4 × 4 cluster as depicted in Figure 1.

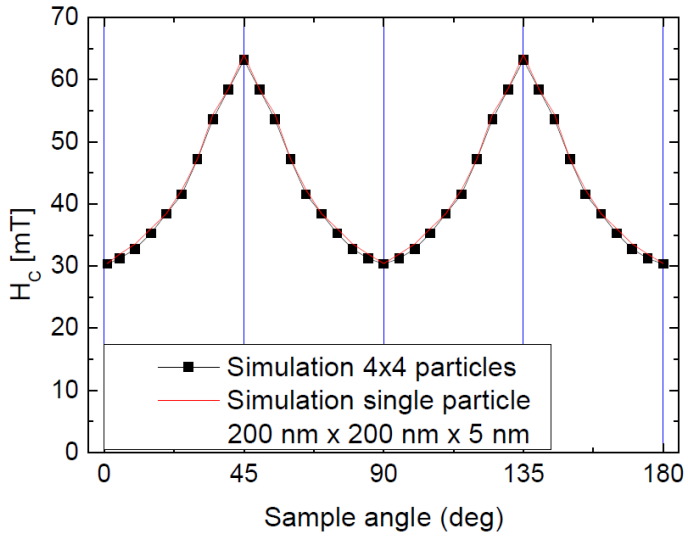

Figure 3. Simulation of single particle with 200 nm side length and 4 × 4 cluster as depicted in Figure 1.

Interestingly, nearly no difference occurs between single object and cluster for this particle dimension. The same finding occurs for the smallest dimension, as visible in Figure 4. For a single particle of 120 nm side length and the respective 4 × 4 cluster, the coercive fields are nearly identical.

The fact that the coercive fields are approximately equal in most cases, especially for the smaller particles, is not sufficient for proving that additional stable states at remanence also occur in the particle clusters under similar conditions as in the single particles. Figure 5 shows hysteresis loops, simulated for a single nanoparticle of 120 nm side length and the respective 4 × 4 cluster, at an

angle of 10° between the particle edge and the external magnetic field. Apparently, the cluster starts reversing its magnetization at smaller fields and finishes this process at larger fields, i.e., the different particles within the cluster switch to another magnetic state at slightly different external magnetic fields. Nevertheless, the plateau between approx. −45 mT and −60 mT, which corresponds to one of the stable intermediate states and leads to one of the additional stable states at remanence when the external magnetic field is reduced to zero [17] is approximately identical.

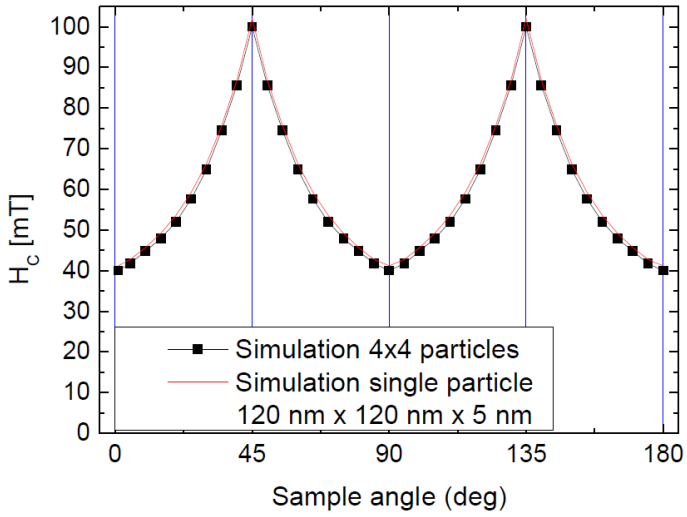

Figure 4. Simulation of single particle with 120 nm side length and 4 × 4 cluster as depicted in Figure 1.

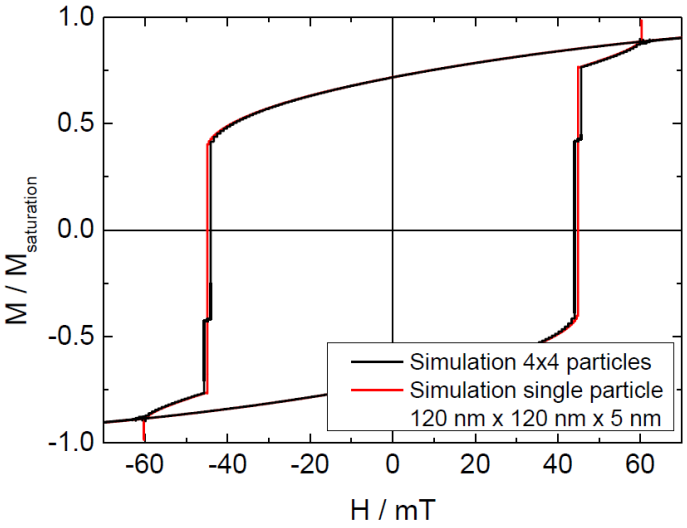

Figure 5. Comparison of hysteresis loops, simulated for a single particle with 120 nm side length and 4 × 4 cluster at 10° angular orientation.

This means that while small deviations of the coercive fields may occur, the most important feature of these particles, i.e., the existence of four stable states at vanishing magnetic field, is not impeded by clustering the single nanoparticles. This finding is supported by the snapshots of the four

magnetization states at zero external magnetic field, depicted in Figure 6. The dimension and angular orientation were chosen identical to Figure 5. The magnetic states shown here were reached by the following field sequences: positive saturation → 0 mT (a), positive saturation → step around −55 mT → 0 mT (b), negative saturation → step around +55 mT → 0 mT (c), and negative saturation → 0 mT (d).

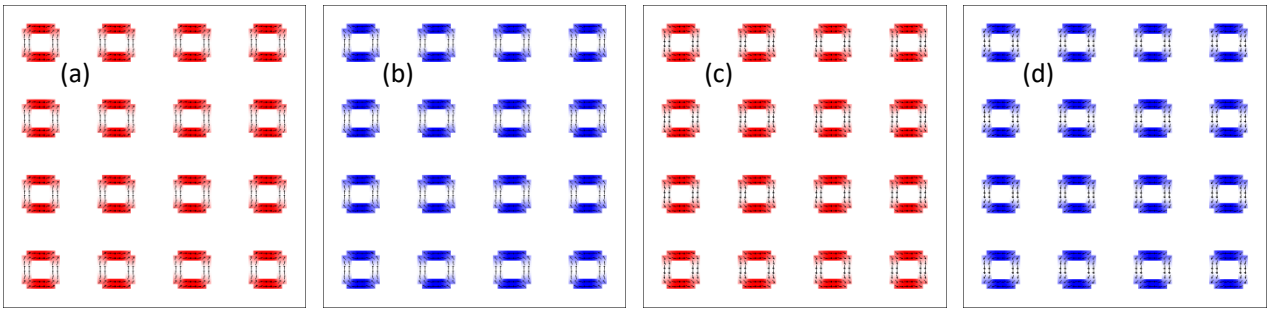

Figure 6. Snapshots of the four possible magnetic states at vanishing external magnetic field, simulated for a cluster of particles with 120 nm side lengths at 10° angular orientation.

The same result was found for all other angles of the three particle sizes in which stable intermediate states occurred.

As these micromagnetic simulations have shown, previous findings of stable magnetic states at remanence can be expanded unambiguously from single magnetic particles to particle clusters. Due to the broadened slopes of the hysteresis loop around the coercive fields, the area of the stable intermediate state (in Figure 5 approx. between −45 mT and −60 mT as well as in the identical positive field range) is slightly reduced which has to be taken into account in technological applications. However, the usual shape deviations in the lithography process results in much stronger limitations of the utilizable field and angular region [19].

4. Conclusions

We have compared magnetic properties and magnetization reversal mechanisms of single magnetic particles of different sizes with clusters prepared from these particles. While the coercive fields near the easy axes of the largest particle showed deviations between single object and cluster, the hysteresis loops of both situations were found to be approximately equal in all other dimensions and angular regions. Especially the possibility to reach a stable magnetic state at remanence from an intermediate "plateau" state is nearly unaltered. This finding ensures that the technological application of such nanoparticles in quaternary memory devices, storing two bits per nanoparticle, can be expanded from single particles to large-area bit-patterned media.

Conflict of Interest

All authors declare no conflicts of interest in this paper.

References

1. Terris BD, Thomson TJ (2005) Nanofabricated and self-assembled magnetic structures as data storage media. *J Phys D Appl Phys* 38: R199–R222.
2. Cowburn RP, Welland ME (2000) Room temperature magnetic quantum cellular automata. *Science* 287: 1466–1468.
3. Akerman J (2005) Toward a universal memory. *Science* 308: 508–510.
4. Bader SD (2006) Colloquium: Opportunities in nanomagnetism. *Rev Mod Phys* 78: 1.
5. Bowden SR, Gibson U (2009) Optical Characterization of All-Magnetic NOT Gate Operation in Vortex Rings. *IEEE T Magn* 45: 5326–5332.
6. Richter H, Dobin A, Heinonen O, et al. (2006) Recording on bit-patterned media at densities of 1Tb/in^2 and beyond. *IEEE T Magn* 42: 2255–2260.
7. Cowburn RP, Koltsov DK, Adeyeye AO, et al. (1999) Single-Domain Circular Nanomagnets. *Phys Rev Lett* 83: 1042.
8. Zhang W, Haas S (2010) Phase diagram of magnetization reversal processes in nanorings. *Phys Rev B* 81: 064433.
9. He K, Smith DJ, McCartney MR (2010) Effects of vortex chirality and shape anisotropy on magnetization reversal of Co nanorings. *J Appl Phys* 107: 09D307.
10. Wang RH, Jiang JS, Hu M (2009) Metallic cobalt microcrystals with flowerlike architectures: Synthesis, growth mechanism and magnetic properties. *Mater Res Bull* 44: 1468–1473.
11. Huang L, Schofield MA, Zhu Y (2010) Control of Double-Vortex Domain Configurations in a Shape-Engineered Trilayer Nanomagnet System. *Adv Mater* 22: 492–495.
12. Thevenard L, Zeng HT, Petit D, et al. (2010) Macrospin limit and configurational anisotropy in nanoscale permalloy triangles. *J Magn Magn Mater* 322: 2152–2156.
13. Moritz J, Vinai G, Auffret S, et al. (2011) Two-bit-per-dot patterned media combining in-plane and perpendicular-to-plane magnetized thin films. *J Appl Phys* 109: 083902.
14. Blachowicz T, Ehrmann A, Steblinski P, et al. (2013) Directional-dependent coercivities and magnetization reversal mechanisms in fourfold ferromagnetic systems of varying sizes. *J Appl Phys* 113: 013901.
15. Blachowicz T, Ehrmann A (2013) Six-state, three-level, six-fold ferromagnetic wire system. *J Magn Magn Mater* 331: 21–23.
16. Blachowicz T, Ehrmann A (2013) Micromagnetic Simulations of Anisotropies in Coupled and Uncoupled Ferromagnetic Nanowire Systems. *Sci World J* 2013: 472597.
17. Blachowicz T, Ehrmann A (2011) Fourfold nanosystems for quaternary storage devices. *J Appl Phys* 110: 073911.
18. Blachowicz T, Ehrmann A (2015) Magnetization reversal modes in fourfold Co nan-wire systems. *J Phys: Conf Ser* 633: 012100.
19. Blachowicz T, Ehrmann A (2016) Stability of magnetic nano-structures with respect to shape modifications. *J Phys: Conf Ser* 738: 012058.
20. Ma CT, Li X, Poon SJ (2016) Micromagnetic simulation of ferrimagnetic TbFeCo films with exchange coupled nanophases. *J Magn Magn Mater* 417: 197–202.
21. Tillmanns A, Oertker S, Beschoten B, et al. (2006) Magneto-optical study of magnetization reversal asymmetry in exchange bias. *Appl Phys Lett* 89: 202512.

22. Donahue MJ, Porter DG (1999) OOMMF User's Guide, Version 1.0. Interagency Report NISTIR 6376, National Institute of Standards and Technology, Gaithersburg, MD.
23. Gilbert TL (2004) A phenomenological theory of damping in ferromagnetic materials. *IEEE T Magn* 40: 3443–3449.
24. Smith N, Markham D, LaTourette J (1989) Magnetoresistive measurement of the exchange constant in varied-thickness permalloy films. *J Appl Phys* 65: 4362.
25. Kneller EF, Hawig R (1991) The exchange-spring magnet: A new material principle for permanent magnets. *IEEE T Magn* 27: 3588–3600.
26. Michea S, Briones J, Palma JL, et al. (2014) Magnetization reversal mechanism in patterned (square to wave-like) Py antidot lattices. *J Phys D Appl Phys* 47: 335001.
27. Ehrmann A, Blachowicz T, Komraus S, et al. (2015) Magnetic properties of square Py nanowires: Irradiation dose and geometry dependence. *J Appl Phys* 117: 173903.
28. Ehrmann A, Komraus S, Blachowicz T, et al. (2016) Pseudo exchange bias due to rotational anisotropy. *J Magn Magn Mater* 412: 7–10.
29. Blachowicz T, Ehrmann A (2016) Square nano-magnets as bit-patterned media with doubled possible data density. *Mater Today: Proceedings*, submitted for publication.

AIMS Press